Study of fully epitaxial Fe/Pt bilayers for spin pumping by ferromagnetic resonance spectroscopy

A. Conca,[1,*] S. Keller,[1] L. Mihalceanu,[1] T. Kehagias,[2] G. P. Dimitrakopulos,[2] B. Hillebrands,[1] and E. Th. Papaioannou[1]

[1]*Fachbereich Physik and Landesforschungszentrum OPTIMAS, Technische Universität Kaiserslautern, 67663 Kaiserslautern, Germany*

[2]*Physics Department, Aristotle University of Thessaloniki, 54124 Thessaloniki, Greece*

(Received 24 November 2015; revised manuscript received 18 February 2016; published 5 April 2016)

We present a study of fully epitaxial Fe/Pt bilayers by means of ferromagnetic resonance (FMR) techniques. The dependence of the resonance field H_{FMR}, the Gilbert damping parameter α, and the FMR linewidth on the Pt thickness is presented and compared with reference layers. Since spin pumping is extremely sensitive to the interface properties, a corresponding study is of large importance. By studying fully epitaxial systems, the existence of an almost perfectly single-crystalline ordered interface is ensured. The measured effects, such as the dependence of the resonant field H_{FMR} on Pt thickness, are thus related to the physics of spin pumping and not to interface disorder effects. The damping parameter α has been extracted from the slope of the linewidth dependence on the FMR frequency. By measuring the enhancement of α with Pt a value for the effective spin mixing conductance of $g_{\mathrm{eff}}^{\uparrow\downarrow} = (4.9 \pm 0.5) \times 10^{19}\,\mathrm{m}^{-2}$ is obtained. We observe an opposite behavior in the dependence of H_{FMR} when compared with reports on YIG/Pt. In addition, the critical role of the proper choice of a reference layer for the estimation of this value is discussed.

DOI: 10.1103/PhysRevB.93.134405

I. INTRODUCTION

The generation of pure spin currents without accompanying charge currents is of large importance for present spintronics and is called to play a critical role in the design of future spintronic devices. The creation and injection of a spin current into a nonmagnetic (NM) material from a ferromagnetic (FM) one is commonly referred to as spin pumping. In spin pumping experiments [1–3], the magnetization of a ferromagnetic layer is typically excited by a microwave field and the generation of the spin current is maximized when the ferromagnetic resonance (FMR) condition is fulfilled. The injected spin current in the NM layer has the form [3]

$$J_{\mathrm{s}} = \frac{\hbar}{4\pi} g^{\uparrow\downarrow} \hat{m} \times \frac{d\hat{m}}{dt}, \tag{1}$$

where $\hat{m}$ is the magnetization unit vector and $g^{\uparrow\downarrow}$ is the spin mixing conductance, which describes the interaction of the spins with the magnetization at the FM/NM interface.

In recent years a large interest in the measurement of spin pumping properties in FM/NM layers with metallic [4–11] and nonmetallic [12–15] FM layers has developed. In many cases the spin current is detected using the inverse spin Hall effect (ISHE) but the presence of spin rectification effects, especially in fully metallic systems, hamper the interpretation of the data. Additional information can be gained with FMR techniques without the disturbance of rectification. Concretely the parameter $g^{\uparrow\downarrow}$ is accessible although the scatter of values in the literature is large.

Here we report on a study of the influence of spin pumping on the FMR properties by using an epitaxial metallic system of Fe(100)/Pt bilayers and discuss the possible origin of the different observed phenomena. Fully epitaxial systems constitute a perfect ordered model with almost ideal and well-defined interfaces. However, the technical difficulty inherent to its deposition has caused most of the research efforts to be focused on polycrystalline materials in metallic systems or epitaxial YIG films with polycrystalline capping layers. In this work we first present a detailed study of the influence of Pt capping layers on the spin pumping properties in a fully ordered system.

II. SAMPLE PREPARATION AND STRUCTURAL CHARACTERIZATION

The samples were deposited by e-beam evaporation on MgO(100) substrates in a MBE chamber with a base pressure $P_b = 5 \times 10^{-10}$mbar. A set of Fe/Pt bilayers with fixed Fe thickness (12 nm) and varying Pt thickness were prepared. Additional reference samples, where Pt is substituted by MgO, MgO/Pt, or Al, have also been prepared. The Fe and Pt films were grown with a deposition rate of 0.05 Å/s. The samples were deposited with a substrate temperature of 300 °C and subsequently annealed at the same temperature.

The characterization by x-ray diffractometry (XRD) (presented elsewhere [11,16]) shows that the Fe/Pt bilayers are fully epitaxial with the Fe unit cell rotated by 45° with respect to the MgO substrate unit cell and with Pt rotated again 45° with respect to Fe. In the case of Fe/Al epitaxial growth of the upper layer could not be demonstrated.

High-resolution transmission electron microscopy (HRTEM) was additionally employed to analyze the Fe/Pt bilayers. Figure 1(a) shows a HRTEM image corresponding to a Fe(12 nm)/Pt(12 nm) sample demonstrating the high crystalline order throughout the bilayer system. The bilayer measured thickness is 23.4 ± 0.34 nm, which is compatible with the nominal value. The surface of the bilayer is very smooth with a measured RMS roughness of 0.3 nm. The roughness of the Fe/Pt interface is slightly larger with a RMS value of 0.9 nm.

Figure 1(b) shows the corresponding common selected area electron diffraction (SAED) pattern, while the specific region around the 020 MgO reflection is shown in detail in Fig. 1(c). Moreover, Fig. 1(d) shows the common SAED pattern with the selected area aperture centered on the deposition side,

*conca@physik.uni-kl.de

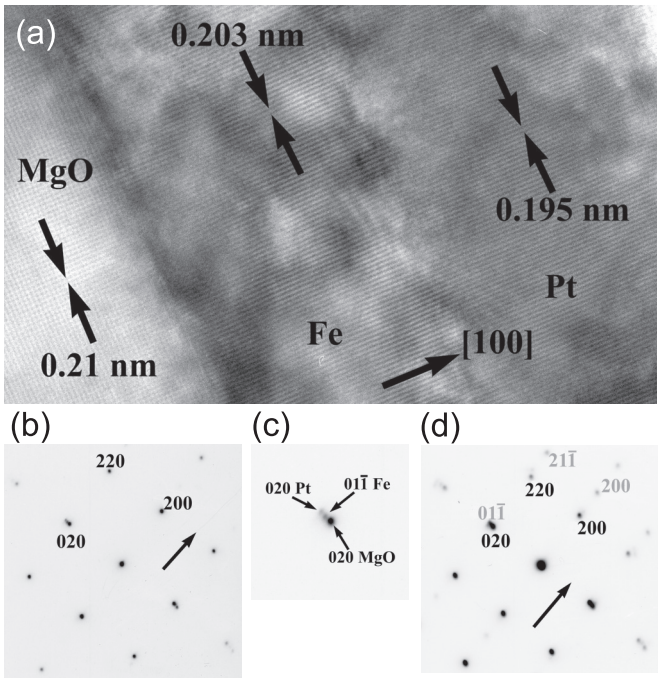

FIG. 1. (a) Cross-sectional HRTEM image of the Fe/Pt bilayer deposited on MgO(100), along the [001] MgO zone axis. The (020) MgO, (01$\bar{1}$) Fe, and (020) crystal planes are perfectly aligned. (b) Corresponding common SAED pattern, dominated by the [001] zone axis of the substrate. The arrow denotes the growth direction. (c) Magnified part of (b) near the 020 MgO reflection, showing the excellent in-plane epitaxy of the three lattices. (d) Common SAED pattern with the aperture placed more at the deposition side, where the [011] zone axis of Fe is revealed parallel to the [001] zone axis of MgO. Gray indices refer to the Fe lattice reflections, while black indices refer to the MgO lattice reflections.

where black and gray indices refer to MgO and Fe reflections, respectively. The above electron diffraction analysis clearly illustrates the excellent epitaxy of the three lattices and confirms that the Fe lattice is in-plane rotated by 45° with respect to both MgO and Pt, as already observed in the XRD measurements. Hence, the [001](100)MgO-Pt‖[011](100)Fe relative epitaxial relationship between the involved lattices is established.

The actual lattice constants for the different materials were extracted from the HRTEM images and SAED patterns. The obtained values are almost identical to the bulk ones implying that the films are stress free. The small in-plane mismatch between the different lattices is accommodated by sparse misfit dislocations. An important conclusion of this data is that, in contrast to other reports [17], no intermixing between the individual layers is observed and therefore the formation of an alloy at the interface can be discarded.

III. FERROMAGNETIC RESONANCE ANALYSIS

The dynamic properties and material parameters were studied by measuring the ferromagnetic resonance using a strip-line vector network analyzer (VNA-FMR). For this, the samples were placed face down and the $\tilde{S}_{12}$ transmission parameter was recorded.

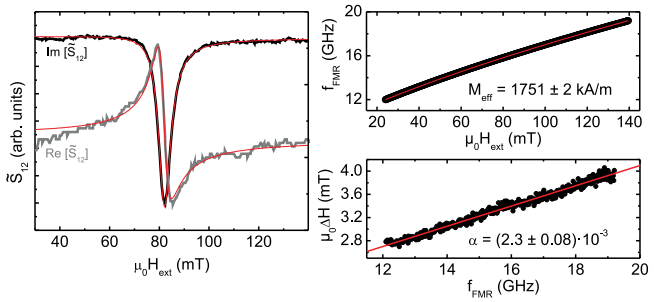

FIG. 2. (a) Example of a FMR spectrum for a Fe(12 nm)/Pt(10 nm) bilayer measured at 14.8 GHz showing the real and imaginary part of the $\tilde{S}_{12}$ transmission parameter. (b) Dependence of the resonance frequency on the applied field for a Fe(12 nm)/MgO(10 nm) reference sample. The red line is a fit to Kittel's formula [19] [Eq. (3)] to extract M_{eff}. (c) Dependence of the resonance linewidth on the frequency for the same sample. The red line is a linear fit to Eq. (4) to determine the Gilbert damping parameter.

Figure 2(a) shows a typical sample FMR spectrum with the real and imaginary part of $\tilde{S}_{12}$ for a Fe(12 nm)/Pt(10 nm) bilayer system for a frequency of 14.8 GHz. Following the approach used by Kalarickal *et al.* [18] the spectra were fitted (red lines) using the expression

$$\tilde{S}_{12}(H_{\text{ext}}) = S_0 + S(H_{\text{ext}})e^{i\phi}$$
$$S(H_{\text{ext}}) = A\frac{1}{H_{\text{FMR}}^2 - H_{\text{ext}}(H_{\text{ext}} - i\Delta H)}, \qquad (2)$$

where H_{ext} is the external applied field, H_{FMR} the resonance field and ΔH is the linewidth. S_0 and A are an offset and a scaling parameter, respectively. ϕ is a phase-shift adjustment parameter. With the extracted data, the dependence of the resonance frequency on the external applied is used to obtain the effective saturation magnetization M_{eff} using Kittel's formula [19] for measurements where H_{ext} is parallel to the easy axis:

$$f_{\text{FMR}} = \frac{|\gamma|\mu_0}{2\pi}\sqrt{(H_{\text{ext}} + H_{\text{ani}})(H_{\text{ext}} + H_{\text{ani}} + M_{\text{eff}})}, \qquad (3)$$

where H_{ani} is the anisotropy field and γ is the gyromagnetic ratio. An example of this is shown in Fig. 2(b) for a Fe/MgO(10nm) reference sample. The Gilbert damping parameter α is accessible via the dependence of the linewidth on the resonance frequency as shown in Fig. 2(c) for the same sample. The red line is a linear fit to

$$\mu_0\Delta H = \mu_0\Delta H_0 + \frac{4\pi\alpha f_{\text{FMR}}}{\gamma}. \qquad (4)$$

Here, ΔH_0 is the inhomogenous broadening and is related to film quality.

IV. ANISOTROPIC PROPERTIES

The study of the in-plane anisotropic properties of the samples was performed by measuring the resonance field H_{FMR} dependence on the azimuthal angle. For the investigation of the anisotropy in thin films, it is also common to measure the magnetization reversal by VSM, SQUID, or MOKE and

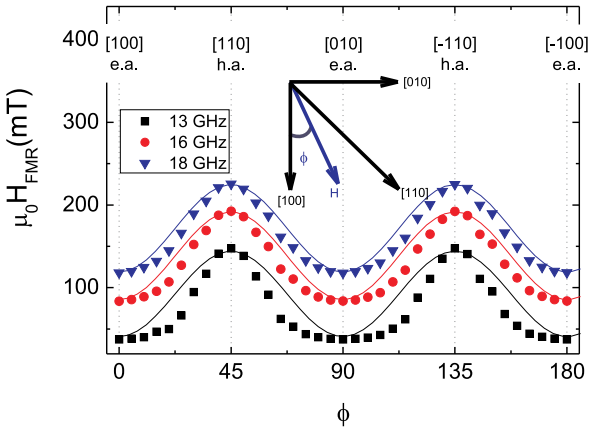

FIG. 3. Dependence of the resonance field H_{FMR} on the azimuthal in-plane angle ϕ for three fixed resonance frequencies for a Fe(12nm)/MgO(10nm) sample. The lines are fits to Eq. (5). The crystallographic Fe directions and the magnetic easy (e.a.) and hard axis (h.a.) are labeled.

use the angular dependence of the coercive field H_C or equivalent parameter to characterize the samples. However, the formation of metastable domain configurations during the reversal process often introduces artifacts, especially for highly ordered epitaxial samples [20,21]. The measurement of H_{FMR} overcomes this problem due to the fact that the film is always in a saturated state.

Figure 3 shows the H_{FMR} angular dependence for three fixed frequencies for a Fe(12 nm)/MgO(10 nm) reference sample. A fourfold anisotropy, as expected for the cubic lattice of Fe can clearly be recognized. Assuming a perfect collinearity between magnetization vector and external field, and with no additional anisotropy contributions, H_{FMR} can be modeled as [22]:

$$\mu_0 H_{FMR} = \mu_0 \tilde{H}_{FMR} + \frac{2K_1}{M_s}\cos(4\phi), \qquad (5)$$

where K_1 is the cubic anisotropy constant, ϕ the in-plane azimuthal angle and $\tilde{H}_{FMR}$ is the averaged resonance field value. The fraction $\frac{2K_1}{M_s}$ is directly the anisotropy field H_{ani}. The lines in Fig. 3 are fits to this formula from which a value of $H_{ani} = 52.4 \pm 0.8$ mT is extracted. Using the known saturation magnetization of Fe, 1750 kA/m (measured for instance by VSM in Ref. [23]), we obtain a value for K_1 of 45850 ± 70 J/m^3. This value is very close to the value of 44500 ± 600 J/m^3 or 39000 J/m^3 reported for thin films [24,25] and still lower than the bulk value [26], 48000 ± 1000 J/m^3. The obtained value for K_1, together with the one extracted from the Kittel fit for this same sample, $M_{eff} = 1751 \pm 2$kA/m, proves the high-quality properties of the films.

In Fig. 3 it is possible to recognize a deviation from the simple $\cos(4\phi)$ behavior. The change of H_{FMR} with the angle around the easy axis is slower than around the hard axis. A similar behavior has been also observed for epitaxial Co(001) films [22] showing also a fourfold anisotropy and it has been attributed to a dragging effect on the magnetization vector towards the easy axis direction. This results in a noncollinearity of the magnetization and external field vectors. The fact that the deviation strongly reduces with increasing frequency (i.e., larger magnetic field) supports this interpretation.

V. THICKNESS DEPENDENCE AND SPIN MIXING CONDUCTANCE

The dependence of the resonance field H_{FMR} on the Pt thickness at a fixed frequency of 13 GHz is shown in Fig. 4(a). Additionally, the values for the reference samples Fe/MgO and Fe/MgO/Pt where spin pumping is suppressed, and for Fe/Al bilayers are shown. The value of H_{FMR} increases compared to the reference samples with increasing Pt thickness until a saturation point around 8–9 nm is reached.

A similar study was reported by Sun *et al.* [12] for YIG/Pt but some differences are observed. First of all, opposite to our results, a decrease is observed for H_{FMR} compared with the samples without Pt. Additionally, the absolute change is at least a factor of two smaller than for Fe/Pt and the saturation

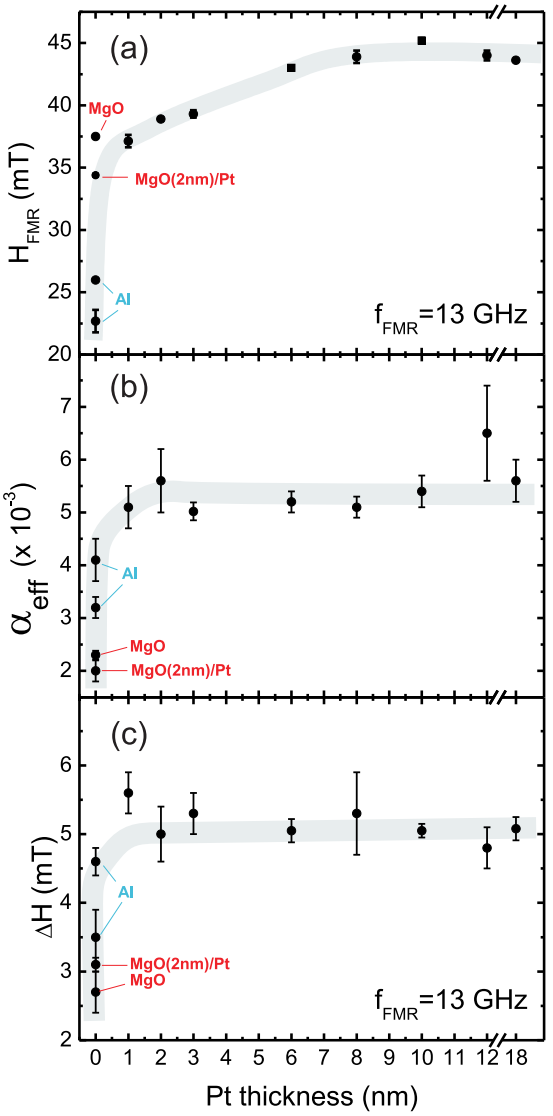

FIG. 4. Dependence of the resonance field H_{FMR} at a fixed frequency (a), the effective damping parameter α_{eff} (b) and the linewidth at a fixed frequency (c) on the Pt thickness for Fe/Pt bilayers. For comparison also the values for the reference samples (Fe/Al, Fe/MgO and Fe/MgO/Pt) are shown. The lines are a guide to the eye.

behavior is observed already for a Pt thickness of 3 nm. In that work, the change of H_{FMR} is attributed to the magnetic proximity effect (MPE), i.e., the apparition of a magnetic ordering in Pt films in contact with ferromagnetic layers. The static coupling between the spins in the Pt atomic layers in the proximity of Fe and the magnetization of Fe itself can generate a shift of the resonance field. However, the fact that the saturation is reached only at a Pt thickness as large as 8–9 nm seems to rule out this possibility in our case since the MPE appears only in the first atomic monolayers [27–30]. Other interfacial effects commonly seen in FM/NM bilayers are known to modify the FMR resonance properties [9]. An additional proof to this is given by the H_{FMR} value for the Fe/Al bilayers, which show an even stronger H_{FMR} shift to smaller values than Fe/Pt (i.e., than YIG/Pt) when compared to Fe/MgO interfaces even though no MPE is present. Still, a pure interfacial effect may not explain why the saturation happens at such a large Pt thickness. The fact that the saturation thickness qualitatively agrees with the estimated spin diffusion length λ_{sd} in Pt (3.5–10 nm) [4,7,10] may hint to a possible relation between the H_{FMR} shift and the dissipation of the injected spin current, i.e., with the magnetic moment generated by the nonequilibrium spin polarization in Pt [31].

Figure 4(b) shows the dependence of the measured effective Gilbert damping parameter α_{eff} on the Pt thickness. The values for the reference samples Fe/MgO and Fe/MgO/Pt and for Fe/Al bilayers are shown. We observe an increase of the measured α_{eff} for the Fe/Pt bilayers compared with the MgO reference layers and a saturation point is found already for the smallest of our Pt thickness (1 nm). It has been already reported that the growth of a Pt layer in contact with a ferromagnetic layer increases the magnetic damping [4,6–12]. This increase is due to several reasons and the measured α_{eff} can be separated into different contributions:

$$\alpha_{eff} = \alpha_0 + \alpha_{mpe} + \alpha_{sp} + \alpha_i. \quad (6)$$

Here α_0 is the intrinsic damping parameter, which can be defined as characteristic of the material under investigation (growth conditions however may influence it strongly) and it is the sum of the losses by magnon-magnon scattering and by energy transfer to the phonon system, α_{mpe} is the contribution due to the dynamic coupling between the ordered spins in Pt due to the MPE and the Fe magnetization, α_{sp} is the result of the losses by the spin current generated in the ferromagnetic layer by the precession of the magnetization and that flows into the Pt layer (spin pumping), and α_i is the increase of damping due to other interfacial effects.

The relative weights of α_{mpe} and α_{sp} in their contribution to α_{eff} is still under discussion in the magnetism community. There are several reasons to affirm that α_{mpe} although present, may not be the dominant contribution in our samples. First of all, the already commented saturation point for the H_{FMR} shift is not fitting with the characteristic scale for this phenomenon. Second, some results in the literature limit the influence of the MPE in metallic FM/Pt bilayers. By inserting a thin metallic and nonmagnetic interlayer with a large spin diffusion length λ_{sd} it is possible to eliminate the MPE without a strong reduction of the injected spin current. Zhang *et al.* [8] showed that the introduction of a thin Cu interlayer in Co/Pt has a reduced impact on the measured spin Hall angle and therefore MPE has only a small influence in the FM/Pt layers. However, a different conclusion can be extracted from data reported elsewhere for the same layer system [10]. There the increase in α_{eff} compared to Co/Al reference samples for Co/Pt is a factor of two larger than for Co/Cu/Pt pointing to similar values for α_{mpe} and α_{sp}. Other studies with NiFe/Pt and CoFeB/Pt and several different metallic interlayers seems to point in the same direction [9].

Figure 4(c) shows the linewidth ΔH of the FMR peak at 13 GHz. This data is obviously directly connected with Fig. 4(b) and shows the same qualitative behavior with a saturation of the value already at $d_{Pt} \sim 1$ nm. For NiFe/Cu/Pt systems [2] (i.e., without MPE), ΔH is reported to show the same behavior with saturation also at $d_{Pt} \sim 1$ nm. Since in this case the MPE is absent, a fast saturation in the change of ΔH (and therefore in α_{eff}) cannot be automatically interpreted as a result of a large α_{mpe} contribution.

The contribution of the spin current dissipation due to spin pumping is related to the spin mixing conductance: [3]

$$\Delta\alpha_{sp} = \frac{\gamma\hbar}{4\pi M_s d_{FM}} g^{\uparrow\downarrow}. \quad (7)$$

It has to be pointed out that this formula is only valid in the case of a Gilbert-like damping, i.e., with $\Delta H \propto f_{FMR}$ as in Eq. (6). This is always the observed situation in our samples. The theoretical description [1,32] of the spin mixing conductance $g^{\uparrow\downarrow}$ for FM/NM interfaces indicates that the value is only defined by the nature of the material used as NM if the role of the interfaces is negligible and for this reason it must be the same for all FM/Pt combinations. However, the relative weights of α_{mpe} and α_{sp} may be different depending on interface quality being the roughness one of the critical parameters. Since the separation of contributions is not possible, it is more correct to speak of an effective spin mixing conductance $g_{eff}^{\uparrow\downarrow}$ for the values obtained using Eq. (7).

In any case, the use of Eq. (7) requires the identification of an adequate reference layer system where the losses by spin pumping and MPE are close to zero allowing for the measurement of the value for α_0. This is a critical point since by the contribution of interfacial effects, α_i can lead to a wrong estimation of $g_{eff}^{\uparrow\downarrow}$. For our estimation we deposited four reference samples corresponding to two kinds of interfaces, Fe/Al and Fe/MgO. For obvious reasons the MPE contribution is zero. Since MgO blocks spin pumping [33] also the contribution α_{sp} vanishes. Both systems [see Fig. 4(b)], the Fe/MgO(10 nm) and the Fe/MgO/Pt show, considering the error bars, the same value for α_{eff}. This value $[(2.15 \pm 0.15) \times 10^{-3}$, average of both systems] is identified as α_0 and it is compatible with literature results [34,35]. The case for the Fe/Al samples is different and shows how important it is to choose a correct reference layer system. Spin pumping is indeed taking place also here but due to the large λ_{sd} of 350–600 nm in Al [36,37], the increase in damping should be negligible and a value close to α_0 is expected. However, as seen in Fig. 4(b), a larger value of $(3.7 \pm 0.5) \times 10^{-3}$ is measured. This can be only a result of the additional interface contributions included in the α_i term.

In recently reported spin pumping studies [9] with NiFe, it was shown that also for this material α_{eff} is different for NiFe/MgO and NiFe/Al, affecting the calculation of $g_{eff}^{\uparrow\downarrow}$.

TABLE I. Comparison of the literature values for the effective spin mixing conductance $g_{\text{eff}}^{\uparrow\downarrow}$ for NM/Pt layer systems. When reported, the reference layer system and the error bar are given.

System	$g_{\text{eff}}^{\uparrow\downarrow}$ (10^{19} m^{-2})	Reference layer	
NiFe/Pt	2.1		Ref. [4]
NiFe/Pt	2.4		Ref. [5]
NiFe/Pt	3.0	Al_2O_3	Ref. [6]
NiFe/Pt	2.5 ± 0.2		Ref. [7]
NiFe/Pt	1.5 ± 0.3		Ref. [8]
NiFe/Pt	6.8 ± 0.6	Al	Ref. [9]
NiFe/Pt	4.9 ± 0.7	MgO	Ref. [9]
CoFeB/Pt	4.0 ± 1.0	MgO,Al	Ref. [9]
Co/Pt	4.0 ± 0.4		Ref. [8]
Co/Pt	8		Ref. [10]
Fe/Pt	3.0 ± 1.0	Al	Ref. [11]
Fe/Pt	2.7 ± 0.8	Al	This work
Fe/Pt	4.9 ± 0.5	MgO, MgO/Pt	This work

Opposite to our case, for NiFe the measured damping is larger for the MgO case. In the case of CoFeB, no difference is observed. This shows again the importance of the choice of the reference layer material.

Since the saturation of α_{eff} takes place already for $d_{\text{Pt}} =$ 1nm, for the calculation of $\Delta\alpha_{\text{eff}}$ we average all the values obtained for the Fe/Pt bilayers. With this a value of $g_{\text{eff}}^{\uparrow\downarrow} = (4.9 \pm 0.5) \times 10^{19}\text{m}^{-2}$ is obtained. Table I shows values obtained for different NM/Pt layer systems and the corresponding reference layer when known. Our value lies in the upper range of the typical values reported for NiFe/Pt bilayers and it is very similar to the values reported for Co/Pt or CoFeB/Pt. Still, the variation of values for $g_{\text{eff}}^{\uparrow\downarrow}$ in the literature is large. We believe that this is due to two main reasons: the different contribution of the interface effects included in the α_{i} term in Eq. (6), also affecting the choice of the reference layer and the different strength of α_{mpe}, which may depend also on interface roughness.

In a previous report of our group a value $g_{\text{eff}}^{\uparrow\downarrow} = (3.0 \pm 1.0) \times 10^{19}\text{m}^{-2}$ was reported for Fe/Pt layers using Fe/Al as reference layer [11]. For the data presented here, a value of $g_{\text{eff}}^{\uparrow\downarrow} = (2.7 \pm 0.8) \times 10^{19}\text{m}^{-2}$ can be calculated by using the Fe/Al bilayers as reference. This value is compatible with the previous study. However, we want to emphasize again that, in our opinion, this value is underestimated and the value obtained with Fe/MgO interfaces as reference is closer to reality. To understand this an important fact has to be remembered. While MgO grows epitaxially on Fe due to the small lattice mismatch, this is not the case for the Al layer. We believe that the difference on the measured spin mixing conductance, when using Al or MgO capped reference layers, reflects the different nature (degree of ordering, metal-to-metal or metal-to-oxide) of the interface. A complete oxidation of the Al capping layer, i.e., the existence of an Fe/Al_2O_3 interface can be discarded since nothing will stop oxygen to react also with Fe. This would have an impact on the measured values of α and M_{eff} much larger than observed.

VI. SUMMARY

A FMR study on the properties dependence on the Pt thickness for fully epitaxial Fe/Pt layers was performed. Both the linewidth and the effective Gilbert damping parameter α_{eff} show an increase when compared with reference Fe/Al, Fe/MgO and Fe/MgO/Pt samples and this increase saturates already for a $d_{\text{Pt}} \approx$ 1nm. This increase is attributed to both magnetic proximity effect and to spin pumping. The resonance field H_{FMR} shows an increase with d_{Pt}, which does not saturate until $d_{\text{Pt}} =$ 8nm, compatible with the spin diffusion length λ_{sd} in Pt pointing to the nonequilibrium magnetization in Pt as the physical origin.

The critical role of the choice of the reference layer for the measurement of the spin mixing conductance has been demonstrated and a value $g_{\text{eff}}^{\uparrow\downarrow} = (4.9 \pm 0.5) \times 10^{19}\,\text{m}^{-2}$ is obtained for the Fe/Pt interface. This value is in agreement with other reports in NM/Pt systems.

ACKNOWLEDGMENTS

Financial support from Carl Zeiss Stiftung and from the PPP-IKYDA 2015-DAAD bilateral German-Greek Collaboration scheme is acknowledged. The authors wish to thank Viktor Lauer and George Vourlias for fruitful discussions.

[1] Y. Tserkovnyak, A. Brataas, and G. E. W. Bauer, Phys. Rev. Lett. **88**, 117601 (2002).
[2] S. Mizukami, Y. Ando, and T. Miyazaki, Phys. Rev. B **66**, 104413 (2002).
[3] Y. Tserkovnyak, A. Brataas, G. E. W. Bauer, and B. I. Halperin, Rev. Mod. Phys. **77**, 1375 (2005).
[4] O. Mosendz, V. Vlaminck, J. E. Pearson, F. Y. Fradin, G. E. W. Bauer, S. D. Bader, and A. Hoffmann, Phys. Rev. B **82**, 214403 (2010).
[5] A. Azevedo, L. H. Vilela-Leão, R. L. Rodríguez-Suárez, A. F. Lacerda Santos, and S. M. Rezende, Phys. Rev. B **83**, 144402 (2011).
[6] M. Obstbaum, M. Härtinger, H. G. Bauer, T. Meier, F. Swientek, C. H. Back, and G. Woltersdorf, Phys. Rev. B **89**, 060407(R) (2014).
[7] Z. Feng, J. Hu, L. Sun, B. You, D. Wu, J. Du, W. Zhang, A. Hu, Y. Yang, D. M. Tang, B. S. Zhang, and H. F. Ding, Phys. Rev. B **85**, 214423 (2012).
[8] W. Zhang, W. Han, X. Jiang, S.-H. Yang, and S. S. P. Parkin, Nature Phys. **11**, 496 (2015).
[9] A. Ruiz-Calaforra, T. Brächer, V. Lauer, P. Pirro, B. Heinz, M. Geilen, A. V. Chumak, A. Conca, B. Leven, and B. Hillebrands, J. Appl. Phys. **117**, 163901 (2015).
[10] J.-C. Rojas-Sánchez, N. Reyren, P. Laczkowski, W. Savero, J. P. Attané, C. Deranlot, M. Jamet, J.-M. George, L. Vila, and H. Jaffrès, Phys. Rev. Lett. **112**, 106602 (2014).
[11] E. Th. Papaioannou, P. Fuhrmann, M. B. Jungfleisch, T. Brächer, P. Pirro, V. Lauer, J. Lösch, and B. Hillebrands, Appl. Phys. Lett. **103**, 162401 (2013).

[12] Y. Sun, H. Chang, M. Kabatek, Y.-Y. Song, Z. Wang, M. Jantz, W. Schneider, M. Wu, E. Montoya, B. Kardasz, B. Heinrich, S. G. E. te Velthuis, H. Schultheiss, and A. Hoffmann, Phys. Rev. Lett. **111**, 106601 (2013).
[13] M. B. Jungfleisch, V. Lauer, R. Neb, A. V. Chumak, and B. Hillebrands, Appl. Phys. Lett. **103**, 022411 (2013).
[14] C. W. Sandweg, Y. Kajiwara, K. Ando, E. Saitoh, and B. Hillebrands, Appl. Phys. Lett. **97**, 252504 (2010).
[15] B. Heinrich, C. Burrowes, E. Montoya, B. Kardasz, E. Girt, Y.-Y. Song, Y. Sun, and M. Wu, Phys. Rev. Lett. **107**, 066604 (2011).
[16] S. Keller, S. Keller, J. Greser, A. Conca, P. Fuhrmann, B. Hillebrands, and E. Th. Papaioannou, Annual Report AG Magnetismus 2015, Technische Universität Kaiserslautern, pp. 99-102, http://www.physik.uni-kl.de/fileadmin/hillebrands/Jahresberichte/Annual_report_2015/AR2015_chapter_4-15.pdf.
[17] Y. Endo, K. Oikawa, T. Miyazaki, O. Kitakami, and Y. Shimada, J. Appl. Phys. **94**, 7222 (2003).
[18] S. S. Kalarickal, P. Krivosik, M. Wu, C. E. Patton, M. L. Schneider, P. Kabos, T. J. Silva, and J. P. Nibarger, J. Appl. Phys. **99**, 093909 (2006).
[19] C. Kittel, Phys. Rev. **73**, 155 (1948).
[20] J. Hamrle, S. Blomeier, O. Gaier, B. Hillebrands, R. Schäfer, and M. Jourdan, J. Appl. Phys. **100**, 103904 (2006).
[21] A. Ruiz-Calaforra, A. Conca, T. Graf, F. Casper, B. Leven, C. Felser, and B. Hillebrands, J. Phys. D: Appl. Phys. **46**, 475001 (2013).
[22] B. Heinrich, J. F. Cochran, M. Kowalewski, J. Kirschner, Z. Celinski, A. S. Arrott, and K. Myrtle, Phys. Rev. B **44**, 9348 (1991).
[23] F. Bonell, S. Andrieu, F. Bertran, P. Lefèvre, A. T. Ibrahimi, E. Snoeck, C. Tiusan, and F. Montaigne, IEEE Trans. Magn. **45**, 3467 (2009).
[24] N. A. Morley, M. R. J. Gibbs, E. Ahmad, I. G. Will, and Y. B. Xu, J. Phys. Condens. Matter **17**, 1201 (2005).
[25] H. Ikeya, Y. Takahashi, N. Inaba, F. Kirino, M. Ohtake, and M. Futamoto, J. Phys.: Conf. Ser. **266**, 012116 (2011).
[26] C. D. Graham Jr., Phys. Rev. **112**, 1117 (1958).
[27] Y. M. Lu, Y. Choi, C. M. Ortega, X. M. Cheng, J. W. Cai, S. Y. Huang, L. Sun, and C. L. Chien, Phys. Rev. Lett. **110**, 147207 (2013).
[28] M. Suzuki, H. Muraoka, Y. Inaba, H. Miyagawa, N. Kawamura, T. Shimatsu, H. Maruyama, N. Ishimatsu, Y. Isohama, and Y. Sonobe, Phys. Rev. B **72**, 054430 (2005).
[29] D. Qu, S. Y. Huang, J. Hu, R. Wu, and C. L. Chien, Phys. Rev. Lett. **110**, 067206 (2013).
[30] F. Wilhelm, P. Poulopoulos, G. Ceballos, H. Wende, K. Baberschke, P. Srivastava, D. Benea, H. Ebert, M. Angelakeris, N. K. Flevaris, D. Niarchos, A. Rogalev, and N. B. Brookes, Phys. Rev. Lett. **85**, 413 (2000).
[31] D. Hou, Z. Qiu, R. Iguchi, K. Sato, K. Uchida, G. E. W. Bauer, and E. Saitoh, arXiv:1503.00816 [cond-mat.mes-hall].
[32] A. Brataas, Y. V. Nazarov, and G. E. W. Bauer, Phys. Rev. Lett. **84**, 2481 (2000).
[33] K. Eid, R. Fonck, M. A. Darwish, W. P. Pratt, and J. Bass, J. Appl. Phys. **91**, 8102 (2002).
[34] M. Oogane, T. Wakitani, S. Yakata, R. Yilgin, Y. Ando, A. Sakuma, and T. Miyazaki, Jpn. J. Appl. Phys. **45**, 3889 (2006).
[35] R. Meckenstock, D. Spoddig, Z. Frait, V. Kambersky, and J. Pelzl, J. Magn. Magn. Mater. **272–276**, 1203 (2004).
[36] F. J. Jedema, M. S. Nijboer, A. T. Filip, and B. J. vanWees, Phys. Rev. B **67**, 085319 (2003).
[37] N. Poli, M. Urech, V. Korenivski, and D. B. Haviland, J. Appl. Phys. **99**, 08H701 (2006).